

12

AD A030933

Comparative Performance of Chemical Lasers with Axisymmetric and Two-Dimensional Nozzles

Aerophysics Laboratory
Laboratory Operations
The Aerospace Corporation
El Segundo, Calif. 90245

27 August 1976

Interim Report

APPROVED FOR PUBLIC RELEASE:
DISTRIBUTION UNLIMITED



Prepared for
NAVAL RESEARCH LABORATORY
Washington, D. C. 20390
SPACE AND MISSILE SYSTEMS ORGANIZATION
AIR FORCE SYSTEMS COMMAND
Los Angeles Air Force Station
P.O. Box 92960, Worldway Postal Center
Los Angeles, Calif. 90009

BY _____
DISTRIBUTION AVAILABLE ONLY CODES

BIG _____ **AVAIL. IN SPECIAL**

A		
---	--	--

UNCLASSIFIED

SECURITY CLASSIFICATION OF THIS PAGE (When Data Entered)

REPORT DOCUMENTATION PAGE		READ INSTRUCTIONS BEFORE COMPLETING FORM
1. REPORT NUMBER ①⑧ SAMS0 TR-76-200	2. GOVT ACCESSION NO.	3. RECIPIENT'S CATALOG NUMBER ⑨
4. TITLE (and Subtitle) ⑥ COMPARATIVE PERFORMANCE OF CHEMICAL LASERS WITH AXISYMMETRIC AND TWO-DIMENSIONAL NOZZLES,		5. TYPE OF REPORT & PERIOD COVERED ⑭ Interim rept.
7. AUTHOR(s) ⑩ Harold Mirels and Walter R. Warren, Jr.		8. CONTRACT OR GRANT NUMBER(s) ⑮ F04701-75-C-0076
9. PERFORMING ORGANIZATION NAME AND ADDRESS The Aerospace Corporation El Segundo, Calif. 90245		10. PROGRAM ELEMENT, PROJECT, TASK AREA & WORK UNIT NUMBERS
11. CONTROLLING OFFICE NAME AND ADDRESS Naval Research Laboratory Washington, D. C. 20390	⑪	12. REPORT DATE 27 August 76
14. MONITORING AGENCY NAME & ADDRESS (if different from Controlling Office) Space and Missile Systems Organization Air Force Systems Command Los Angeles, Calif. 90009	⑫ 25p.	13. NUMBER OF PAGES 17
		15. SECURITY CLASS. (of this report) Unclassified
16. DISTRIBUTION STATEMENT (of this Report) Approved for public release; distribution unlimited.		19. DECLASSIFICATION/DOWNGRADING SCHEDULE
17. DISTRIBUTION STATEMENT (of the abstract entered in Block 20, if different from Report)		
18. SUPPLEMENTARY NOTES		
19. KEY WORDS (Continue on reverse side if necessary and identify by block number) Chemical Laser Performance Chemical Laser Nozzle Design Chemical Laser Modeling		
20. ABSTRACT (Continue on reverse side if necessary and identify by block number) Saturated output power from cold-reaction cw HF/DF diffusion-type chemical lasers in which axisymmetric or two-dimensional oxidizer nozzles are used is compared for the case where the pumping reaction is fast compared with collisional deactivation. For typical HF laser flow conditions and $p_w > 5$ Torr cm, the axisymmetric nozzle has an output power twice that of a two-dimensional nozzle with the same exit flow, exit pressure p , and exit semiwidth w . In this p_w regime, however,		

DDC
REF ID: A67112
OCT 19 1976
REGISTERED
C

DD FORM 1473
(FACSIMILE)

409367

UNCLASSIFIED

SECURITY CLASSIFICATION OF THIS PAGE (When Data Entered)

UNCLASSIFIED

SECURITY CLASSIFICATION OF THIS PAGE(When Data Entered)

19. KEY WORDS (Continued)

20. ABSTRACT (Continued)

the chemical efficiency of the axisymmetric nozzle is 20%, or less, that of a premixed ($p_w = 0$) laser. For $p_w = 1$ Torr cm, the axisymmetric nozzle has about 30% greater output than the corresponding two-dimensional nozzle and a chemical efficiency equal to about 60% that of a premixed laser. For $p_w < 0.5$ Torr cm, both nozzles have essentially premixed laser performance.

UNCLASSIFIED

SECURITY CLASSIFICATION OF THIS PAGE(When Data Entered)

PREFACE

The present study was supported by NAVSEA HEL project PMS-405 through U.S. Air Force Space and Missile Systems Organization (SAMSO) Contract No. F04701-75-C-0076.

CONTENTS

PREFACE	1
I. INTRODUCTION	5
II. ANALYSIS	7
III. CONCLUDING REMARKS	17
NOMENCLATURE	19

FIGURES

1. Exit Geometry for Axisymmetric and Two-Dimensional F/He Nozzles with Characteristic Diffusion Distance w	8
2. Simplified Mixing Model	9
3. Variation of Output Power $\bar{P}_e(j = 1/2)$ with Diffusion Rate Parameter $\zeta_D^{1/2}$ for Laminar Flow and $K_1 \rightarrow \infty$	15

I. INTRODUCTION

In continuous diffusion-type cold-reaction HF chemical lasers being investigated, H_2 is diffused into supersonic jets that contain F and a diluent such as He.¹ Analytical studies of these devices have assumed that the F/He jets are generated by two-dimensional nozzles.²⁻⁵ It is of interest to consider configurations in which axisymmetric nozzles are used because these may permit improved laser performance. Hence, the two-dimensional chemical laser model of Ref. 4 is generalized here to include axisymmetric flow. Saturated laser output power is determined for both laminar and turbulent mixing. The performance of chemical lasers with two-dimensional and axisymmetric nozzles is then compared. Nozzle wall viscous effects are neglected.

¹D. J. Spencer, H. Mirels, and D. A. Durran, "Performance of CW HF Chemical Laser with N_2 or He Diluent," J. Appl. Phys. 43 (3), 1151 (1972).

²R. Hofland and H. Mirels, "Flame Sheet Analyses of CW Diffusion-Type Chemical Lasers, I. Uncoupled Radiation," AIAA J. 10 (4), 420 (1972).

³R. Hofland and H. Mirels, "Flame Sheet Analyses of CW Diffusion-Type Chemical Lasers, II. Coupled Radiation," AIAA J. 10 (10), 1271 (1972).

⁴H. Mirels, R. Hofland, and W. S. King, "Simplified Model of CW Diffusion-Type Chemical Lasers," AIAA J. 11 (2), 156 (1973).

⁵J. E. Broadwell, "Effect of Mixing Rate on HF Chemical Laser Performance," Appl. Opt. 13 (4), 962 (1974).

II. ANALYSIS

We consider both axisymmetric and two-dimensional F/He nozzles. These are illustrated in Fig. 1. H_2 is added along the perimeter of the axisymmetric nozzle and along the sides of the two-dimensional nozzle.

In the simplified model of Ref. 4, it is assumed that the reactants are premixed. However, the reaction does not begin until the reactants reach a prescribed "flame sheet" location, which is denoted by $r_f = r_f(x)$ in Fig. 2. Unless otherwise specified, the notation herein is the same as in Ref. 4. We consider a saturated laser wherein $I \rightarrow \infty$, $g \rightarrow 0$, and the output power per unit volume gl remains finite. The variation of output power, with stream-wise distance, for the stream tube that enters the flame sheet at (x_0, r_0) is, from Eq. (9b) of Ref. 4,

$$\frac{2B}{\sigma k_{cd}[F]_0} gl = (1 + k_1) e^{-k_f(x-x_0)/u} - 1 \quad (1)$$

Let P denote the net laser output power generated up to station x per half nozzle of unit height and per nozzle for two-dimensional and axisymmetric flows, respectively. The value of dP/dx is found by integrating the contribution of all the reacted stream tubes between $r = r_f(x)$ and $r = w$. Thus

$$\frac{dP}{dx} = (2\pi)^j \int_{r_f(x)}^w gl r^j dr \quad (2a)$$

where $j = 0, 1$ for the two-dimensional and axisymmetric nozzles, respectively. Let $R = r_f(x)/w$ and $R_0 = r_f(x_0)/w$.

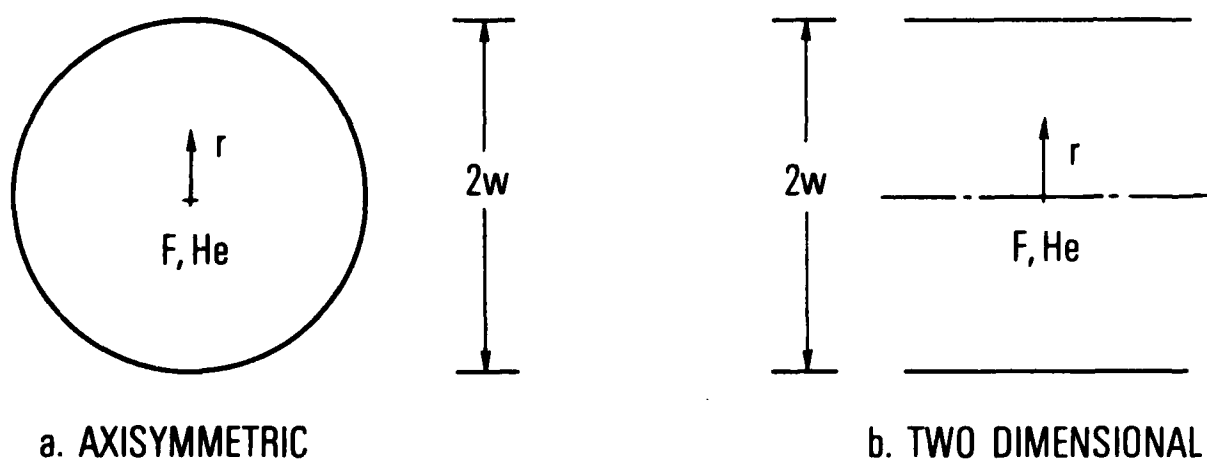


Figure 1. Exit Geometry for Axisymmetric and Two-Dimensional F/He Nozzles with Characteristic Diffusion Distance w

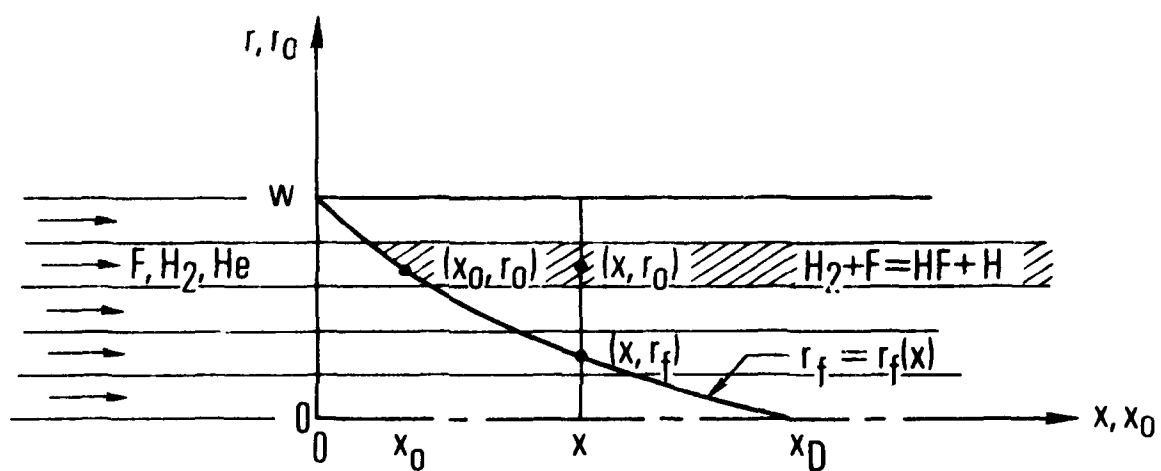


Figure 2. Simplified Mixing Model

Also, introduce

$$\bar{P} = \frac{2P}{\epsilon u [F]_0 \pi^j w^{1+j}} \quad (2b)$$

where \bar{P} is the ratio of P to the output power that would be obtained if one photon is generated for each pair of initial F atoms. (The latter output power occurs in a saturated premixed laser in the limit $K_1 \rightarrow \infty$.) Substitution of Eq. (1) into Eq. (2) and introduction of nondimensional variables yields

$$\frac{d\bar{P}}{d\zeta} = (-1)(1 + K_1) \int_0^\zeta e^{-K_1(\zeta - \zeta_0)} \frac{dR_0^{j+1}}{d\zeta_0} d\zeta_0 - 1 + R^{j+1} \quad (3)$$

where $\zeta = x k_{cd}/u$ is the ratio of streamwise distance x to the characteristic collisional deactivation distance u/k_{cd} . Further integration yields

$$\begin{aligned} \bar{P} = \frac{1 + K_1}{K_1} & \left[\int_0^\zeta e^{-K_1(\zeta - \zeta_0)} \frac{dR_0^{j+1}}{d\zeta_0} d\zeta_0 + 1 - R^{j+1} \right] \\ & + \int_0^\zeta R_0^{j+1} d\zeta_0 - \zeta \end{aligned} \quad (4)$$

As ζ increases, P increases, reaches a maximum, and then decreases. The maximum value of P is denoted P_e and occurs at a station denoted ζ_e . The quantity P_e represents the saturated laser output power, and ζ_e is the length of the lasing region. ζ_e occurs at a station where $dP/d\zeta = 0$, or where $dP/d\zeta$ changes discontinuously from a positive to a negative value.

Equations (3) and (4) simplify in the limit $K_1 \rightarrow \infty$. Note that the major contribution to the integrals occurs near $\zeta = \zeta_0$. Evaluating the coefficient

of $e^{-K_1(\zeta - \zeta_0)}$ at $\zeta_0 = \zeta$ in these integrals, integrating, and taking the limit $K_1 \rightarrow \infty$, we obtain

$$\frac{d\bar{P}}{d\zeta} = -dR^{j+1}/d\zeta - 1 + R^{j+1} \quad (5)$$

and

$$\bar{P} = \int_0^\zeta R_o^{j+1} d\zeta_o - \zeta + 1 - R^{j+1} \quad (6)$$

These expressions can be evaluated when R is specified.

In the present study, we assume

$$R = 1 - (\zeta/\zeta_D)^N \quad \zeta < \zeta_D \quad (7a)$$

$$= 0 \quad \zeta > \zeta_D \quad (7b)$$

for both two-dimensional and axisymmetric nozzles. Here, $N = 1/2, 1$ for laminar and turbulent diffusion, respectively, and ζ_D is the value of ζ at which the flame sheet reaches the nozzle centerline.

It is assumed here that, for given exit flow conditions, and a given value of w , the value of ζ_D is the same for both two-dimensional and axisymmetric nozzles. For the two-dimensional nozzles, Eqs. (7) agree with the flame sheet shape used previously in Ref. 4. For the axisymmetric nozzles, the mixing is essentially two dimensional when $\zeta/\zeta_D \ll 1$. Hence, the use of Eqs. (7) with the same value of ζ_D for both two-dimensional and axisymmetric nozzles is clearly valid when $\zeta_e/\zeta_D \ll 1$. As ζ/ζ_D increases, the rate at which H_2 diffuses into the F/He stream tends to be more rapid for the axisymmetric than for the two-dimensional nozzle because of transverse curvature effects. This feature of the mixing process is not modeled here.

For simplicity, we obtain closed-form results for $K_1 \rightarrow \infty$, although similar closed-form expressions can be obtained for finite values of K_1 . In order to display the dependence of the dependent variables on j and N , we introduce the notation $\zeta_e(j, N)$, $\bar{P}_e(j, N)$.*

The quantity $\zeta_e(j, N)$ is found by setting Eq. (5) equal to zero or observing the value of ζ at which $dP/d\zeta$ changes discontinuously from a positive to a negative value. This procedure yields

$$\zeta_e(0, N) = N \quad \zeta_D > N \quad (8a)$$

$$= \zeta_D \quad \zeta_D < N \quad (8b)$$

$$\zeta_e(1, 1/2) = (1/2) \left[1 - (\zeta_e/\zeta_D)^{1/2} (1 - \zeta_e) \right] \quad (8c)$$

$$= \zeta_D \left\{ 1 - \zeta_e \left[2 - (\zeta_e/\zeta_D)^{1/2} \right] \right\}^2 \quad (8d)$$

$$\zeta_e(1, 1) = 1 + \zeta_D - (1 + \zeta_D^2)^{1/2} \quad (8e)$$

Equations (8c) and (8d) are solved by iteration, with (8c) used for $\zeta_D > 1/2$ and (8d) for $\zeta_D < 1/2$. Initial estimates are $\zeta_e = 1/2$ in Eq. (8c) and $\zeta_e = \zeta_D$ in Eq. (8d). Except for Eq. (8b), the above expressions correspond to stations where $dP/d\zeta = 0$ and $\zeta_e/\zeta_D < 1$. For these cases, lasing terminates before the flame sheet reaches the nozzle centerline. Equation (8b)

* In Ref. 4, the quantity $\bar{P}_e(j, N)$ is denoted by the symbol η and is a measure of chemical efficiency.

corresponds to the case in which lasing is terminated by the arrival of the flame sheet at the nozzle centerline. The corresponding laser output power is

$$\bar{P}_e(0, N) = (N/\zeta_D)^N / (N + 1) \quad \zeta_D > N \quad (9a)$$

$$= 1 - \zeta_D / (N + 1) \quad \zeta_D < N \quad (9b)$$

$$\bar{P}_e(1, N) = 2 \left(\frac{\zeta_e}{\zeta_D} \right)^N \left[1 - \frac{\zeta_e}{N + 1} \right] - \left(\frac{\zeta_e}{\zeta_D} \right)^{2N} \left[1 - \frac{\zeta_e}{2N + 1} \right] \quad (9c)$$

For given values of ζ_D and N , Eq. (9c) can be evaluated by substituting the value of ζ_e obtained from Eqs. (8c), (8d), or (8e). In the limit $\zeta_D^N \gg 1$, Eqs. (8) and (9) indicate

$$\zeta_e(1, N) = N \left[1 - \frac{1}{2} \left(\frac{N}{\zeta_D} \right)^N + O \left(\frac{N}{\zeta_D} \right)^{4N-1} \right] \quad (10a)$$

$$\bar{P}_e(1, N) = \frac{2}{N + 1} \left(\frac{N}{\zeta_D} \right)^N \left[1 - \frac{(N + 1)^2}{2(2N + 1)} \left(\frac{N}{\zeta_D} \right)^N + O \left(\frac{N}{\zeta_D} \right)^{2N} \right] \quad (10b)$$

These equations provide, explicitly, the dependence of $\zeta_e(1, N)$ and $\bar{P}_e(1, N)$ on ζ_D for ζ_D large.

Equations (8) and (9) have been evaluated numerically and the results are presented in Table 1. The variation of $\bar{P}_e(j, 1/2)$ with $\zeta_D^{1/2}$ is indicated in Fig. 3. The quantity $\bar{P}_e(0, N)/\bar{P}_e(1, N)$ in Table 1 can be interpreted as the ratio of two-dimensional to axisymmetric nozzle output power for cases where both nozzles have the same exit flow conditions and the same semi-width w . For small values of ζ_D^N , both nozzles have the same output power.

Table 1. Output Power \bar{P}_e and Length of Lasing Region ζ_e for $K_1 \rightarrow \infty$

ζ_D^N	$j = 0$										$j = 1$									
	$N = 1/2$					$N = 1$					$N = 1/2$					$N = 1$				
	\bar{P}_e	ζ_e	\bar{P}_e	ζ_e	\bar{P}_e	\bar{P}_e	ζ_e	\bar{P}_e	ζ_e	\bar{P}_e	\bar{P}_e	ζ_e	\bar{P}_e	ζ_e	\bar{P}_e	ζ_e	\bar{P}_e	ζ_e	\bar{P}_e	ζ_e
0.1	0.993	0.01	0.950	0.1	0.992	0.010	0.936	0.095	1.001	1.015										
0.2	0.973	0.04	0.900	0.2	0.968	0.037	0.877	0.180	1.005	1.026										
0.4	0.893	0.16	0.800	0.4	0.888	0.120	0.772	0.323	1.006	1.036										
0.6	0.760	0.36	0.700	0.6	0.792	0.201	0.685	0.434	0.960	1.022										
0.8	0.589	0.50	0.600	0.8	0.700	0.264	0.613	0.519	0.841	0.979										
1.0	0.471	0.50	0.500	1.00	0.622	0.308	0.552	0.586	0.757	0.906										
2.0	0.236	0.50	0.250	1.00	0.384	0.405	0.363	0.764	0.614	0.689										
4.0	0.118	0.50	0.125	1.00	0.213	0.454	0.212	0.877	0.554	0.590										
6.0	0.079	0.50	0.083	1.00	0.147	0.470	0.149	0.917	0.537	0.557										
8.0	0.059	0.50	0.0625	1.00	0.112	0.477	0.115	0.938	0.527	0.543										
10.0	0.047	0.50	0.050	1.00	0.091	0.482	0.094	0.950	0.516	0.555										
20.00	0.024	0.50	0.025	1.00	0.046	0.491	0.048	0.975	0.522	0.521										

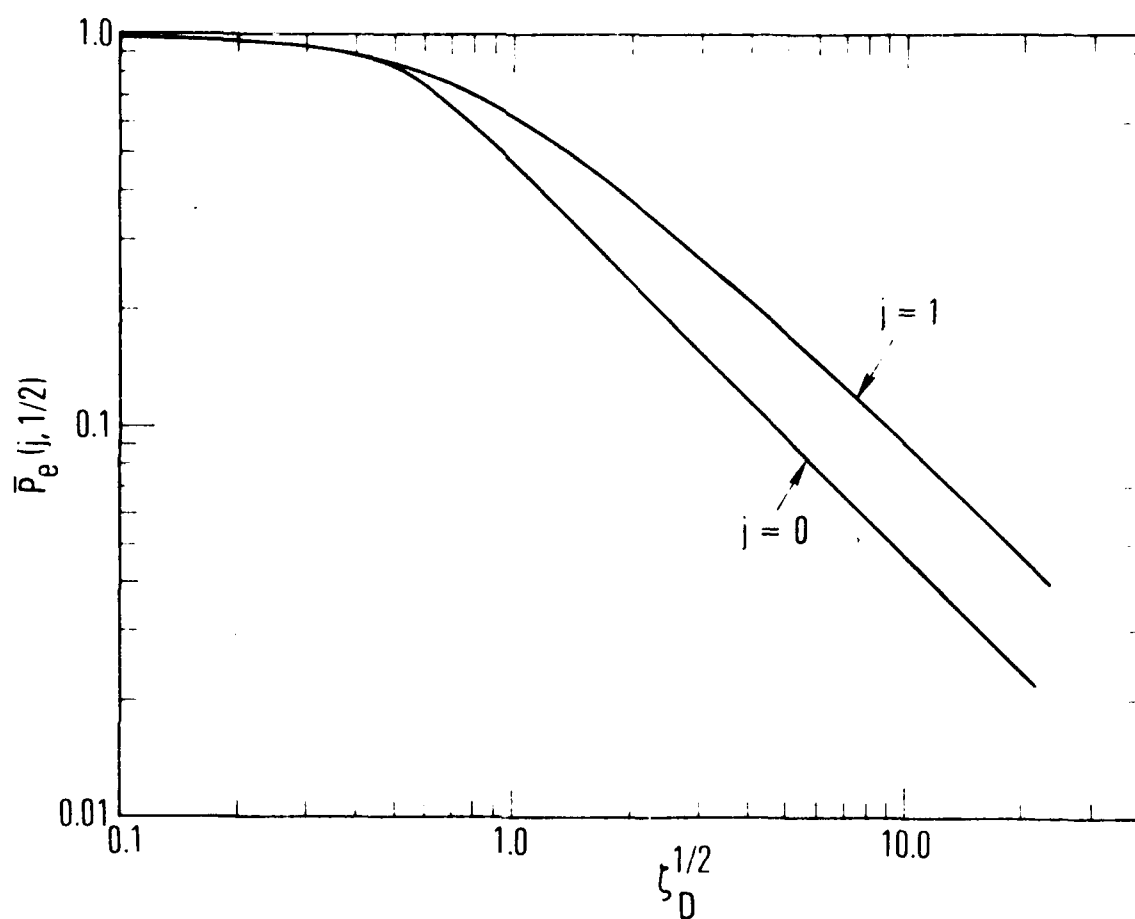


Figure 3. Variation of Output Power $\bar{P}_e(j = 1/2)$ with Diffusion Rate Parameter $\zeta_D^{1/2}$ for Laminar Flow and $K_1 \rightarrow \infty$

In these cases, the diffusion is fast, relative to the deactivation, and the performance is similar to that for a premixed laser. For ζ_D^N large, the two-dimensional nozzle has one-half the output power of the axisymmetric nozzle because only the small portion of the F/He stream in direct contact with the bounding H_2 stream lases. Since the "wetted perimeter" is twice as large for the axisymmetric as for the two-dimensional nozzle, the output power from the former is twice as great as that from the latter. The output power, however, is relatively low in this region. The ratio of two-dimensional to axisymmetric output power is slightly larger than 1 for values of ζ_D^N between 0.1 and 1.0. This is probably because the same flame sheet shape was assumed for corresponding axisymmetric and two-dimensional flows. In reality, the axisymmetric diffusion rate is faster than the two-dimensional diffusion rate, which should cause the ratio of two-dimensional to axisymmetric output power to be ≤ 1 for all ζ_D^N . Both the two-dimensional and the axisymmetric nozzles have similar performance in the region $0.1 \leq \zeta_D^N \leq 1.0$, and a more accurate description of the diffusion process appears unwarranted, particularly for laminar diffusion, which is the case of primary interest.

III. CONCLUDING REMARKS

Approximate expressions for ζ_D^N are given by Eqs. (44) of Ref. 4. For a HF laser with laminar flow and a helium diluent

$$\zeta_D^{1/2} = 3.27 \frac{p(\text{Torr}) w(\text{cm})}{(p/p_F)^{1/2}} \left[\frac{2}{A} \left(\frac{400}{T} \right)^{1.385} \right] \quad (11a)$$

where p is the static pressure, and p_F is the partial pressure of the fluorine at the nozzle exit. Equation (11a) neglects the effect of combustion-generated deactivators. For typical flow conditions ($p/p_{HF} = 10$, $T = 400$ K, $A = 2$)

$$\zeta_D^{1/2} = p(\text{Torr}) w(\text{cm}) \quad (11b)$$

For this flow condition, a saturated laser, $K_1 \rightarrow \infty$, and $pw > \text{Torr cm}$, i.e., $\zeta_D^{1/2} > 5$, the axisymmetric nozzle has an output power twice that of a two-dimensional nozzle with the same exit flow conditions and exit width w . In this pw regime, however, the chemical efficiency of the axisymmetric nozzle is 20% or less that of a premixed ($pw = 0$) laser. For $pw = 1$ Torr cm, i.e., $\zeta_D^{1/2} = 1$, the axisymmetric nozzle has about 30% greater output than the corresponding two-dimensional nozzle and a chemical efficiency equal to about 60% that of a premixed laser. For $pw < 0.5$ Torr cm, i.e., $\zeta_D^{1/2} < 0.5$, both nozzles have essentially premixed laser performance. For either nozzle, a reduction in pw results in improved performance (Fig. 3). The effect of $p/p_F \pm 10$ is found from Eq. (11a).

Fabrication and nozzle wall boundary layer effects also have to be considered when comparing two-dimensional and axisymmetric nozzles. These are beyond the scope of this study.

NOMENCLATURE

B	σ/ϵ
$[F]_0$	initial atomic fluorine concentration, moles/cc
g	local gain, $\sigma[\eta_u - \eta_l]$
I	net local intensity
j	0, 1 for two-dimensional and axisymmetric nozzles, respectively.
K_1	k_f/k_{cd}
k_{cd}	collisional deactivation rate (sec^{-1})
k_f	forward pumping rate (sec^{-1})
N	1/2, 1 for laminar and turbulent mixing, respectively
P	output power up to station x, Eq. (2a)
\bar{P}	normalized output power up to station x, Eq. (2b)
$\bar{P}_e(j, N)$	normalized net laser output power
p	static pressure at nozzle exit
R, R_0	$r_f(x)/w, r_f(x_0)/w$
r	radial ordinate, Fig. 2
$r_f(x)$	flame sheet location, Fig. 2
u	streamwise velocity
w	nozzle exit semiwidth, Fig. 1
x, x_0	streamwise distance, Fig. 2
x_D	characteristic diffusion distance, Fig. 2
ϵ	energy per mole of photons
ζ	normalized streamwise distance, xk_{cd}/u

ζ_D normalized diffusion distance, $x_D k_{cd}/u$
 $\zeta_e(j, N)$ normalized length of lasing region, $x_e k_{cd}/u$
 σ cross section for stimulated emission, cm^2/mode

LABORATORY OPERATIONS

The Laboratory Operations of The Aerospace Corporation is conducting experimental and theoretical investigations necessary for the evaluation and application of scientific advances to new military concepts and systems. Versatility and flexibility have been developed to a high degree by the laboratory personnel in dealing with the many problems encountered in the nation's rapidly developing space and missile systems. Expertise in the latest scientific developments is vital to the accomplishment of tasks related to these problems. The laboratories that contribute to this research are:

Aerophysics Laboratory: Launch and reentry aerodynamics, heat transfer, reentry physics, chemical kinetics, structural mechanics, flight dynamics, atmospheric pollution, and high-power gas lasers.

Chemistry and Physics Laboratory: Atmospheric reactions and atmospheric optics, chemical reactions in polluted atmospheres, chemical reactions of excited species in rocket plumes, chemical thermodynamics, plasma and laser-induced reactions, laser chemistry, propulsion chemistry, space vacuum and radiation effects on materials, lubrication and surface phenomena, photo-sensitive materials and sensors, high precision laser ranging, and the application of physics and chemistry to problems of law enforcement and biomedicine.

Electronics Research Laboratory: Electromagnetic theory, devices, and propagation phenomena, including plasma electromagnetics; quantum electronics, lasers, and electro-optics; communication sciences, applied electronics, semiconducting, superconducting, and crystal device physics, optical and acoustical imaging; atmospheric pollution; millimeter wave and far-infrared technology.

Materials Sciences Laboratory: Development of new materials; metal matrix composites and new forms of carbon; test and evaluation of graphite and ceramics in reentry; spacecraft materials and electronic components in nuclear weapons environment; application of fracture mechanics to stress corrosion and fatigue-induced fractures in structural metals.

Space Sciences Laboratory: Atmospheric and ionospheric physics, radiation from the atmosphere, density and composition of the atmosphere, aurorae and airglow; magnetospheric physics, cosmic rays, generation and propagation of plasma waves in the magnetosphere; solar physics, studies of solar magnetic fields; space astronomy, x-ray astronomy; the effects of nuclear explosions, magnetic storms, and solar activity on the earth's atmosphere, ionosphere, and magnetosphere; the effects of optical, electromagnetic, and particulate radiations in space on space systems.

THE AEROSPACE CORPORATION
El Segundo, California